Journal of Green Energy Research and Innovation

Thermal Behavior of R134a Droplet in Dropwise Condensation Considering Marangoni Convection Flow on Horizontal and Vertical Surfaces for Refrigeration Systems

Loghman Mohammadpour, Hesam Moghadasi

Highlights

- **The impacts of Marangoni convection, contact angle and surface orientation in refrigerant R134a droplet on DWC utilizing CFD tools are evaluated.**
- **The influences of Ma number on temperature distribution and average heat flux across horizontal and vertical surfaces are assessed.**
- **The vertical surface delivers about 4.5% greater average heat flux than the horizontal one at $Ma = 11020$ and $\theta = 110°$.**
- **The findings offer refrigeration focused insights that can help reduce energy consumption.**

Graphical Abstract

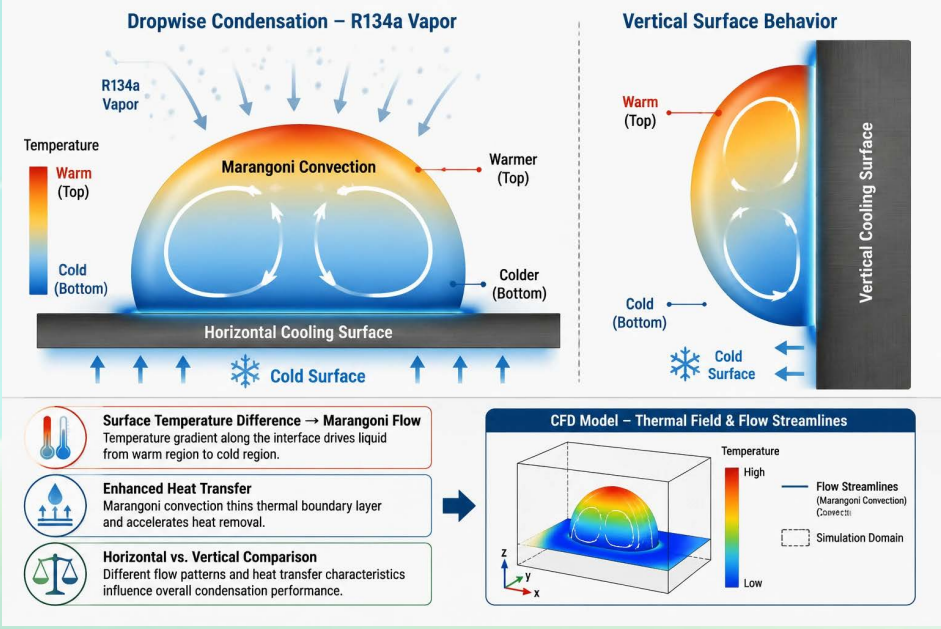

Use your device to scan and read the article online

Citation

L. Mohammadpour and H. Moghadasi, "Thermal Behavior of R134a Droplet in Dropwise Condensation Considering Marangoni Convection Flow on Horizontal and Vertical Surfaces for Refrigeration Systems," *Journal of Green Energy Research and Innovation*, vol. 3, no. 2, pp. 78-89, 2026.

https://doi.org/10.61186/jgeri.3.2.78

Journal of Green Energy Research and Innovation 3.2 (2026) 78-89

Online ISSN: 3041-9018

Journal of Green Energy Research and Innovation

Journal Homepage: www.jgeri.araku.ac.ir

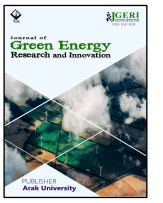

Thermal Behavior of R134a Droplet in Dropwise Condensation Considering Marangoni Convection Flow on Horizontal and Vertical Surfaces for Refrigeration Systems

Loghman Mohammadpour [1], Hesam Moghadasi [2,*]

[1] *School of Mechanical Engineering, Iran University of Science and Technology (IUST), 16846-13114, Tehran, Iran.*

[2] *Department of Mechanical Engineering, Faculty of Engineering, Arak University, Arak, 38156-88349, Iran.*

A R T I C L E I N F O

Keywords:
CFD,
DWC,
Marangoni Convection,
R134a Droplet,
Horizontal and Vertical Surfaces.

Article History:
Received: 26 December 2025;
Revised: 01 February 2026;
Accepted: 16 April 2026.

Article type:
Research Article

* ***Corresponding authors***
E-mail address
h-moghadasi@araku.ac.ir (H. Moghadasi)

A B S T R A C T

Dropwise condensation (DWC) increases phase change heat transfer efficiency, enabling more energy efficient thermal processes that directly support greener energy technologies and help lower overall carbon emissions. Correspondingly, this research work presents a numerical assessment of isolated R134a droplet during DWC on solid surfaces, focusing on the coupled impacts of Marangoni convection, contact angle across horizontal ($\beta = 0°$) and vertical ($\beta = 90°$) surfaces to investigate their impact on heat transfer during DWC. In this regard, droplet geometry was modeled utilizing Surface Evolver, while computational fluid dynamics (CFD) simulations were performed in ANSYS FLUENT with a pressure-based solver and Semi-Implicit Method for Pressure-Linked Equations (SIMPLE) algorithm. The simulation outcomes were validated through comparison with established theoretical models and previously published experimental measurements. Regarding the results, greater Marangoni numbers (Ma) enhance internal circulation, leading to more uniform temperature distributions and increased heat transfer coefficients. Also, contact angle was found to positively influence average heat flux (AHF) by reducing liquid–solid contact area, while vertical surfaces consistently exhibited higher AHF because of smaller droplet footprints. The results indicate that at $Ma = 11020$ and $\theta = 110°$, the vertical surface yields an AHF that is nearly 4.5% superior than that of the horizontal surface. Furthermore, unlike previous studies, which primarily examined these phenomena in general condensation contexts, this work specifically addresses their implications for refrigeration systems. By investigating R134a droplets, the findings provide novel insights into droplet scale condensation mechanisms that can contribute to reducing energy consumption in refrigerators.

1. Introduction

Condensation refers to the phase transition process in which vapor transforms into liquid when it comes into contact with a solid surface whose temperature is lower than that of the surrounding vapor environment [1-3]. When the surface temperature falls below the saturation temperature corresponding to the vapor pressure, vapor molecules lose energy and begin to accumulate on the surface in liquid form. This physical phenomenon is widely encountered in both natural environments and engineered systems and represents one of the most important mechanisms of phase-change heat transfer. Because condensation involves the release of latent heat, it plays a crucial role in thermal transport processes and significantly influences the efficiency of many energy conversion and thermal management technologies. From a large-scale engineering perspective, condensation processes are fundamental in several industrial sectors. In power generation systems, particularly in steam power plants, condensation is a key stage of the thermodynamic cycle where exhaust steam from turbines is condensed in condensers to recover water and maintain low turbine back pressure, thereby improving cycle efficiency [4].

Similarly, condensation mechanisms are central to water desalination technologies such as thermal distillation, where vaporized seawater must condense efficiently to produce fresh water [5]. In addition, many thermal control and heat recovery systems rely on condensation to remove heat effectively from working fluids [6]. At smaller technological scales, condensation is also essential in devices used in everyday life. Refrigeration systems and air-conditioning units operate based on vapor compression cycles in which the working refrigerant condenses after releasing heat to the surroundings [7,8]. The effectiveness of the condensation stage directly influences the overall performance and energy efficiency of these systems. Condensation on solid surfaces generally occurs in two primary modes: dropwise condensation (DWC) and filmwise condensation (FWC) [9,10]. These two modes differ significantly in terms of liquid distribution and heat transfer characteristics. In the dropwise condensation regime, vapor condenses into numerous discrete droplets that form and grow on the surface [11]. The droplets remain separated from one another and periodically detach or slide away, allowing new droplets to form on freshly exposed surface areas. This continuous renewal of the condensing surface minimizes the thermal resistance between the vapor and the solid substrate. As a result, DWC is widely recognized as a highly efficient mode of phase-change heat transfer. Enhanced heat transfer performance during DWC can significantly improve the efficiency of thermal systems, which is particularly important in the context of sustainable energy technologies and efforts aimed at reducing global carbon emissions. As condensation proceeds, individual droplets gradually increase in size due to direct condensation and droplet coalescence. When neighboring droplets merge, they can form larger droplets that eventually create a continuous liquid layer covering the surface. This transition marks the onset of filmwise condensation. In the FWC mode, a stable liquid film develops on the surface, which acts as a thermal barrier between the vapor and the solid wall. Because heat must then be conducted through this liquid layer, the overall heat transfer resistance increases substantially. Numerous experimental and theoretical investigations have demonstrated that heat transfer coefficients during DWC can be several times higher than those observed in FWC, making dropwise condensation the preferred mode for many heat transfer applications [12]. Given the significant thermal advantages of DWC, considerable research efforts have been directed toward increasing the probability of maintaining this mode on condensing surfaces. One widely adopted approach involves modifying the surface properties of the substrate in order to reduce its surface energy, thereby encouraging droplet nucleation and preventing the formation of continuous liquid films [13,14]. This objective can be achieved through the application of promoter layers or ultrathin coatings that alter the wettability characteristics of the surface. Such coatings are typically extremely thin and introduce minimal additional thermal resistance, which is why their influence on heat conduction through the surface is often considered negligible [15,16]. The heat transfer performance associated with dropwise condensation is influenced by a variety of physical and geometric parameters. Among the most important factors are the contact angle between the liquid droplet and the solid surface, which determines droplet shape and wettability behavior [17], the inclination angle of the surface relative to gravity [18], the micro- and nano-scale texture of the surface [19], and the thermophysical properties of the condensing liquid such as viscosity, surface tension, and thermal conductivity [20]. Each of these parameters affects droplet dynamics, including nucleation, growth, coalescence, and departure from the surface. The role of surface inclination in condensation heat transfer has been examined in several experimental studies. For example, Tancon et al. [21] conducted a comparative investigation of condensation on horizontal and vertical surfaces. Their experimental findings indicated that vertical surfaces exhibited approximately 40% higher heat transfer rates compared with horizontal configurations, and about a 10% improvement relative to surfaces inclined at $\beta = 45^{\circ}$. The enhanced performance observed on vertical surfaces was mainly attributed to more efficient droplet removal due to gravitational forces. In another study, Baghel et al. [22] analyzed the heat transfer characteristics of individual droplets beneath surfaces with different thermal resistances. Their results showed that the overall heat transfer rate remained nearly identical for droplets with a deformed geometry and those exhibiting an ideal spherical cap shape. Inclined surfaces frequently appear in practical thermal systems. A common example can be observed in domestic refrigeration units, where condensation often takes place on both horizontal and vertical internal walls. Improving condensation heat transfer in such systems can lead to noticeable gains in energy efficiency and operational performance. Some investigations [23] have reported that increasing the inclination angle can enhance the heat transfer rate for water droplets because gravity assists droplet movement and removal. However, this improvement becomes less significant for relatively small droplets ($V < 20$ μL) and for inclination angles below approximately 45°, where gravitational effects are comparatively weak. Another important mechanism affecting heat transfer during dropwise condensation is Marangoni convection [24]. In a stationary droplet attached to a solid surface, a temperature difference typically exists between the liquid–vapor interface and the substrate. This temperature difference generates a thermal gradient along the droplet surface. Since surface tension is a temperature-dependent property, variations in temperature along the interface lead to spatial variations in surface tension. These gradients induce tangential stresses along the interface that drive fluid motion within the droplet, creating internal circulation patterns commonly referred to as Marangoni flow. This internal flow mechanism can influence heat transfer in two competing ways: it may introduce additional thermal resistance by redistributing temperature fields, or it may enhance convective heat transport inside the droplet, thereby improving the overall heat transfer rate [25]. The intensity of Marangoni convection is typically characterized using the Marangoni number (Ma), a dimensionless parameter that represents the relative importance of surface tension–driven convection compared with diffusive transport mechanisms. The Marangoni number is defined according to Equation (1) and provides a useful metric for evaluating the influence of interfacial temperature gradients on droplet dynamics and heat transfer behavior during dropwise condensation [26].

$$Ma = -\frac{d\sigma}{dT}\frac{\Delta T\, C_P\, L\, \rho}{k\, \mu} \tag{1}$$

In Equation (1), the parameter dσ/dT represents the variation of surface tension with respect to temperature, commonly referred to as the surface tension gradient. The term ΔT indicates the temperature difference established between the vapor phase and the condensation surface, which acts as a driving force for the condensation process. Additionally, several thermophysical properties of the liquid droplet are incorporated into the formulation.

Specifically, L denotes the height of the droplet formed on the condensing surface, while ρ corresponds to the liquid density. The parameter μ represents the dynamic viscosity of the liquid, reflecting the internal resistance of the fluid to flow, and k indicates the thermal conductivity of the liquid, which characterizes its ability to conduct heat. Together, these parameters describe the physical and thermal characteristics of the droplet that influence the condensation behavior represented in Equation (1). Furthermore, the internal flow within the droplet is directed from regions of lower surface tension gradient (corresponding to higher temperatures) toward regions of greater surface tension gradient (lower temperatures). This behavior is characteristic of Marangoni convection. Figure 1 illustrates the resulting flow pattern inside a liquid droplet resting on a solid surface.

In a numerical study, Phadnis and Rykaczewski [1] assessed the impact of Marangoni convection on heat transfer. Their findings indicated that this convection mechanism enhances heat transfer, although the impact is noteworthy only for droplets with radii below 100 μm. A review of the literature reveals extensive research on the effects of inclination angle and Marangoni convection on heat transfer during DWC. However, few studies have specifically addressed these phenomena in the context of refrigeration systems. To bridge this gap, the present research numerically examines R134a, one of the most commonly utilized refrigerants, with the aim of contributing to energy efficiency improvements in refrigerators. In this study, numerical simulations were conducted for an isolated liquid droplet on both horizontal ($\beta = 0°$) and vertical ($\beta = 90°$) surfaces. Surface Evolver was utilized to model the droplet geometry on the inclined surfaces, while ANSYS FLUENT was employed to perform the computational fluid dynamics (CFD) simulations and attain the thermal outcomes. Besides, the effects of contact angle and Marangoni convection were systematically analyzed.

2. Physical Model

2.1. Arrangement

To initiate examination of single droplets on solid surfaces process, an accurate simulation of droplet behavior on the surface is essential. Two primary approaches are commonly utilized to model droplet shapes: the two-circle approximation [2] and the Surface Evolver [3] method. The former requires manual geometric construction based on analytical calculations, whereas the latter now more extensively adopted relies on computational modeling. Surface Evolver is an interactive software tool designed to simulate the geometry and energy of surfaces influenced by surface tension and other forces. It iteratively evolves the surface toward a minimal energy configuration, typically minimizing surface area under given constraints. In this work, a liquid R134a droplet on a solid surface was simulated at inclination angles of 0° and 90°, with contact angles of 100° and 110°. Figure 2 depicts the droplet configuration for $\beta = 0°$ and $\theta = 110°$. To promote DWC, the solid surface was coated with a boosted promoter layer. The thermo-physical features of the R134a droplet as well as, solid substrate, and promoter layer are reported in Tables 1 and 2, respectively.

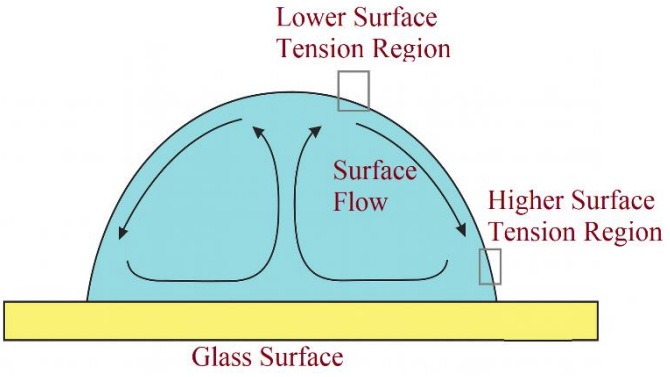

Figure 1. Marangoni flow inside a liquid droplet.

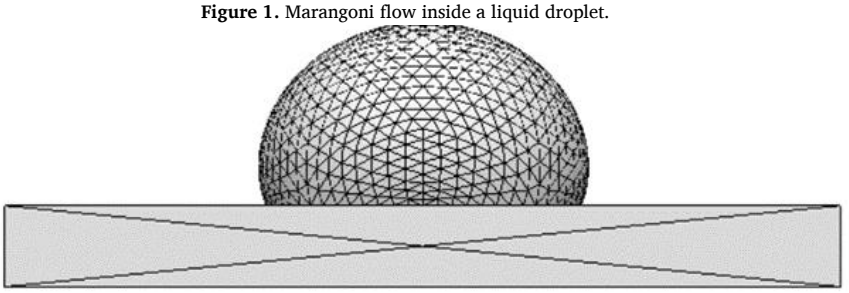

Figure 2. Schematic of a simulated liquid droplet on a solid surface in Surface Evolver with θ = 110°; β = 0°; V = 20μl and ρ_l = 1207 kg/m^3.

Table 1. Thermo-physical properties of R134a droplet [4,5].

Properties	Value	Unit
Pr	2.94	-
C_P	837	$J/kg\ K$
T_{sat}	280	K
T_w	270	K
ρ_l	1207	kg/m^3
ρ_v	31.2	kg/m^3
h_{lv}	134.8	kJ/kg
σ	0.0046	N/m
k	0.082	$W/m\ K$
M	102.03	$kg/kmol$
μ	0.198	$gr/cm\ s$
$\hat{\sigma}$	0.01	-

Table 2. Thermo-physical features of the condensing surface and drop promoter layer [6].

Sub-Domain	Material	Density (kg/m3)	Specific Heat (J/kg K)	Thermal Conductivity (W/m K)	Thickness (μm)
Surface	Al	2702	879.04	180	1000
Promoter Layer	Long Chain Hydrocarbon Coating	764.64	3100	0.05	0.1

2.2. Mathematical Framework

In the present work, the fluid within the droplet is assumed to behave as an incompressible medium, meaning that its density remains constant throughout the flow field. Additionally, the influence of viscous dissipation on the thermal energy balance is considered negligible and therefore omitted from the governing equations. Under these assumptions, the transport phenomena occurring within the droplet are described using the three fundamental conservation laws of fluid mechanics: conservation of mass, conservation of momentum, and conservation of energy. These governing relations are formulated in the Cartesian coordinate system to facilitate numerical implementation. The equations are discretized and solved using the Finite Volume Method (FVM), which is widely employed in computational fluid dynamics due to its strong conservation properties and robustness in handling complex geometries and boundary conditions. The simplified mathematical expressions corresponding to the continuity, momentum, and energy equations are presented in Equations (2) to (4). Equation (2) represents the continuity equation, which enforces mass conservation within the fluid domain. This relation indicates that, for an incompressible fluid, the divergence of the velocity field must be zero, ensuring that the mass flow entering any control volume is equal to the mass flow leaving it. Equation (3) describes the momentum conservation equation derived from the Navier–Stokes equations. This equation accounts for the temporal variation of momentum, the convective transport of momentum, the pressure gradient forces acting within the fluid, viscous diffusion effects, and the influence of body forces such as gravity. Equation (4) corresponds to the energy conservation equation, which governs the temperature distribution within the droplet. This equation represents the balance between transient heat storage, convective heat transport caused by fluid motion, and thermal diffusion due to temperature gradients.

$$\frac{\partial u_i}{\partial x_i} = 0 \tag{2}$$

$$\frac{\partial u_i}{\partial t} + \frac{\partial u_j u_i}{\partial x_i} = -\frac{1}{\rho}\frac{\partial P}{\partial x_i} + \frac{\mu}{\rho}\frac{\partial u_i}{\partial x_i^2} + g_i \tag{3}$$

$$\frac{\partial T}{\partial t} + \frac{\partial u_i T}{\partial x_i} = \alpha \frac{\partial^2 T}{\partial x_i^2} \tag{4}$$

Moreover, in order to find the exact magnitude of the capillary temperature (T_{cap}), Equation (5) can be utilized:

$$T_{cap} = T_{sat}\left(1 - \frac{2\sigma}{r h_{lv} \rho}\right) \tag{5}$$

where T_{sat} represents the saturation temperature of the working fluid, σ denotes the surface tension at the liquid–vapor interface, and r corresponds to the radius of the condensed droplet. In addition, h_{lv} refers to the latent heat of vaporization, which characterizes the amount of energy required for the phase change process, while ρ indicates the density of the liquid phase. These parameters collectively describe the thermophysical properties that govern droplet formation and heat transfer behavior during condensation.

Furthermore, in order to determine the heat transfer coefficient at the droplet interface, denoted by h_i, the formulation provided in Equation (6) is utilized, as reported in [7]. This expression enables a more accurate evaluation of interfacial heat transfer by accounting for the relevant fluid properties and interfacial conditions.

$$h_i = \left(\frac{2\hat{\sigma}}{2-\hat{\sigma}}\right)\left(\frac{h_{lv}^2 \Delta\rho}{T_{sat}}\right)\left(\frac{M}{2\pi \bar{R}\, T_{sat}}\right)^{0.5}\left(1-\frac{P_v}{\Delta\rho 2 h_{lv}}\right) \quad (6)$$

In Equation (6), $\hat{\sigma}$ represents the condensation coefficient, which characterizes the effectiveness of the phase change process occurring at the liquid–vapor interface. The term P_v corresponds to the vapor pressure evaluated at the dew point temperature, reflecting the thermodynamic state of the vapor during condensation. Furthermore, the parameter $\Delta\rho$ indicates the density difference between the liquid and vapor phases, a quantity that significantly influences condensation dynamics and droplet behavior. In addition, M denotes the molecular weight of the vapor, while $\bar{R}$ represents the universal gas constant. These thermophysical parameters are incorporated into Equation (6) to properly characterize the interfacial heat and mass transfer processes associated with vapor condensation.

2.3. Numerical Solution and Boundary Conditions

In this study, the transient three-dimensional Navier–Stokes equations together with the energy conservation equation are solved simultaneously in a coupled framework in order to accurately capture the fluid flow and heat transfer processes occurring within the system. Considering the unsteady nature of droplet behavior and thermal interactions, the governing equations are treated in their time-dependent form, allowing the evolution of velocity, pressure, and temperature fields to be properly represented throughout the computational domain.

For the thermal boundary conditions, a Dirichlet condition is prescribed on the solid surface, where the wall temperature is fixed and expressed as $T = T_W$. This assumption implies that the temperature of the inclined substrate remains constant during the condensation process, thereby providing a controlled thermal environment for droplet formation and heat transfer.

At the interface between the liquid droplet and the surrounding medium, a mixed boundary condition is imposed to represent the heat exchange between the droplet and its environment. Specifically, a Robin boundary condition is applied in which the heat transfer coefficient is defined as $HTC = h_i$. In addition to this convective heat transfer formulation, a temperature constraint is enforced at the interface, expressed as $T = T_{cap}$, which represents the characteristic temperature at the droplet cap. These boundary conditions collectively describe the thermal interaction between the droplet surface and the ambient vapor phase.

The overall configuration of these boundary conditions for a liquid droplet resting on an inclined surface is illustrated in Figure 3. This figure provides a schematic representation of the computational domain and clearly identifies the locations where the specified thermal constraints and interfacial conditions are applied. Such a boundary specification enables a more realistic simulation of the droplet heat transfer and fluid dynamics on inclined surfaces.

To numerically solve the governing equations, a pressure-based computational fluid dynamics solver available in ANSYS FLUENT was utilized. Within this framework, the spatial discretization of the convective terms was carried out using a second-order upwind scheme. The use of this higher-order discretization approach improves the accuracy of the numerical solution by reducing numerical diffusion and providing a more precise representation of gradients in velocity, pressure, and temperature fields throughout the computational domain. In addition, the coupling between the pressure and velocity fields was handled using the Semi-Implicit Method for Pressure-Linked Equations (SIMPLE) algorithm. This algorithm is widely applied in pressure-based solvers to iteratively enforce mass conservation while updating the pressure and velocity distributions. Through this procedure, the pressure correction equation is solved to adjust the velocity field, ensuring that the continuity equation is satisfied at each iteration. The combined use of the second-order upwind discretization scheme and the SIMPLE pressure–velocity coupling approach enhances the stability and reliability of the numerical solution for the fluid flow and heat transfer processes considered in this study.

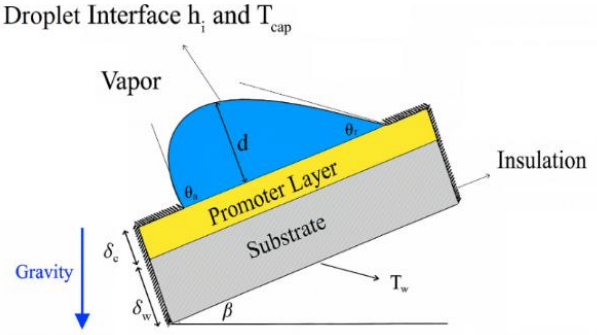

Figure 3. Applied boundary conditions on the studied domain for a droplet on an inclined surface.

2.4. Grid Independence Evaluation

Mesh generation plays a critical role in computational accuracy and efficiency, as it directly affects both simulation time and the quality of outcomes. In this examination, ANSYS ICEM CFD, a commercial meshing software, was employed to generate an optimal mesh for the computational domain. Also, Figure 4 exhibits the resulting grids for the liquid droplet on an inclined solid surface, viewed from diverse angles. It is crucial to mention that, the meshes are unstructured and composed of tetrahedral elements.

As illustrated in Figure 5, a mesh independence study was carried out to ensure that the numerical results are not influenced by the discretization of the computational domain. In this evaluation, the temperature distribution inside the liquid droplet was examined along the droplet height while it was positioned on an inclined solid surface. By comparing the temperature profiles obtained from several mesh configurations with different element densities, the sensitivity of the solution to grid refinement was carefully investigated. The analysis showed that further refinement beyond a certain grid resolution produced negligible changes in the predicted temperature distribution. Based on this comparison, a computational mesh containing approximately 1.2 million elements was selected for the remaining simulations. This grid density was found to provide sufficiently accurate results while maintaining a reasonable computational time. Consequently, the chosen mesh offers an appropriate compromise between numerical accuracy and computational efficiency, ensuring reliable simulation outcomes without imposing unnecessary computational cost.

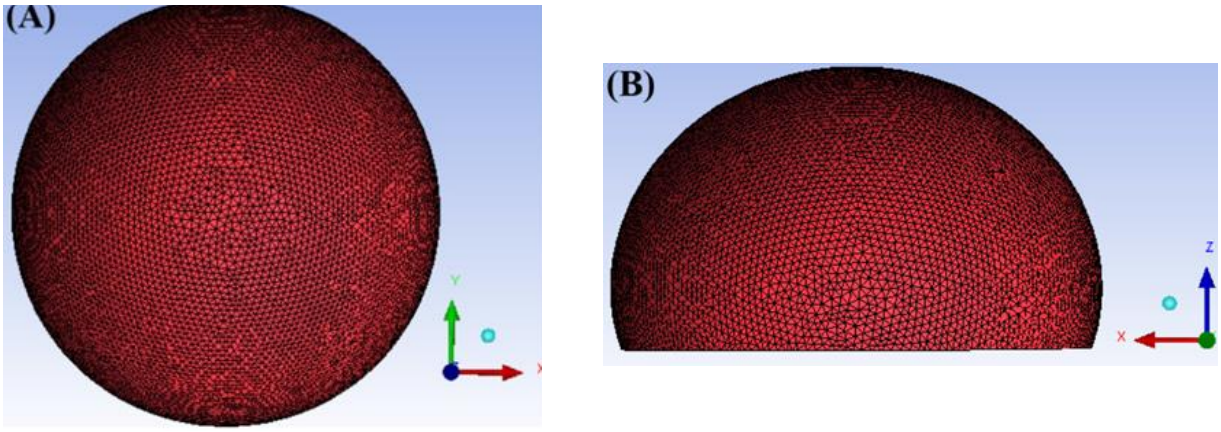

Figure 4. The generated grid for a liquid droplet on an inclined surface with β = 0° at different perspectives, (A) X-Y plane (Z = 0) (B) X-Z plane (Y = 0).

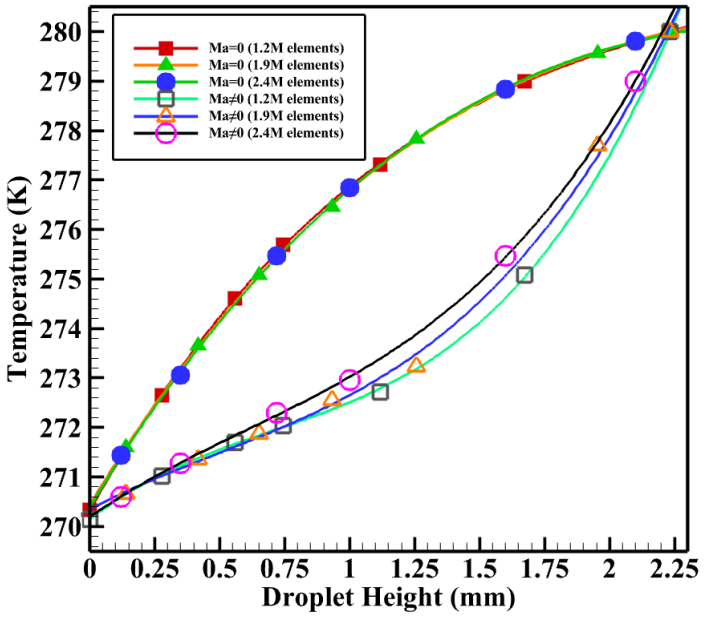

Figure 5. Temperature profile at midline of droplet (X-Y plane, Z = 0) versus droplet height for various grid sizes ranging from 1.2 to 2.4 million element. Considering, contact angle (θ) = 110°, V = 20 µl, T_{sat} = 280 K, ΔT = 10 K, $\hat{\sigma}$ = 0.01, δ_w = 1 mm, δ_c = 10 µm, K_c = 0.2W/m K and K_w = 180W/m K.

2.5. Validation

The validation of this study was carried out through two complementary approaches. First, the droplet shape generated considering Surface Evolver was compared with experimental observations reported by Annapragada et al. [8]. As demonstrated in Figure 6, the simulated droplet profile closely matches the experimental data, representing strong agreement and confirming the reliability of the Surface Evolver based modeling. Second, the findings attained from the CFD simulations were validated against both theoretical predictions and experimental findings from the literature. This dual validation approach reinforces the credibility of the numerical framework employed in this research.

To evaluate the average heat flux (AHF) associated with a single droplet, Baghel et al. [22] performed a theoretical investigation in which a liquid droplet with a volume of V = 3.59 μl was analyzed at different contact angles. In the present study, an identical droplet configuration was reproduced using Surface Evolver under the same physical conditions to ensure a consistent comparison. The obtained droplet geometry and associated characteristics were then compared with the results reported by Baghel et al. As illustrated in Figure 7(a), the comparison indicates a strong level of agreement between the two studies, confirming that the implemented approach can accurately capture the droplet shape and its geometric characteristics. In addition to this validation step, further verification of the numerical model was carried out by comparing the CFD predictions with available experimental data reported by Rajkumar et al. [33]. In their experimental work, the authors investigated the influence of subcooling on the heat transfer coefficient associated with an individual droplet during the condensation process. Their observations demonstrated that the heat transfer coefficient gradually decreases as the degree of subcooling increases, highlighting the sensitivity of droplet heat transfer performance to thermal conditions. To ensure a meaningful comparison, the same droplet configuration and operating conditions considered in the experimental study were replicated in the present simulations. The resulting numerical predictions for the heat transfer coefficient were then compared with the corresponding experimental measurements reported by Rajkumar et al. As depicted in Figure 7(b), the comparison reveals a satisfactory level of agreement between the CFD results and the experimental data. This consistency between numerical and experimental findings provides additional confidence in the validity and reliability of the adopted numerical methodology and confirms that the implemented modeling framework is capable of accurately predicting the thermal behavior of individual droplets under varying subcooling conditions.

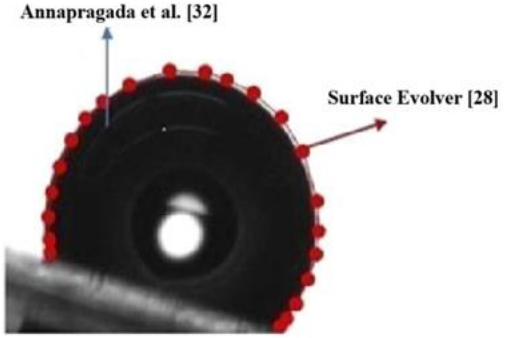

Figure 6. The comparison of the obtained simulated droplet shape from Surface Evolver with an experimental work for a liquid water droplet with $\beta = 15°$, $V = 10\ \mu l$ and $T_{sat} = 313\ K$.

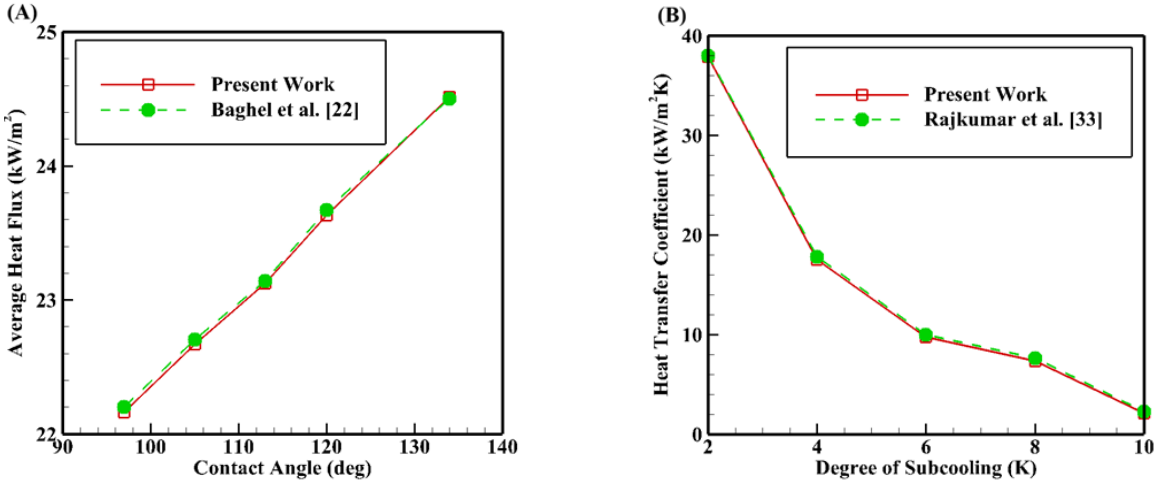

Figure 7. Validation of the current solution with the data of (a) Baghel et al. [9] at $V = 3.59\ \mu l$, $T_{sat} = 313K$, $\Delta T = 10\ K$, $\hat{\sigma} = 0.04$ and $\beta = 0°$ (b) Rajkumar et al. [10] at $V = 10\ \mu l$ and $\beta = 0°$.

3. Result and Discussion

The present research scrutinizes the combined impacts of the Ma number and contact angle on heat transfer rate and internal temperature distribution within an individual liquid droplet. In addition, simulations were executed for droplets on both horizontal ($\beta = 0°$) and vertical ($\beta = 90°$) surfaces to capture the influence of surface orientation.

3.1. The Impacts of Ma Number on AHF for an Individual Droplet across Horizontal and Vertical Surfaces

As mentioned previously, Marangoni convection plays an important role in influencing the heat transfer characteristics during DWC. This phenomenon arises due to gradients in surface tension along the liquid–vapor interface, which are typically induced by temperature differences across the droplet surface. Such variations generate tangential stresses that drive fluid motion within the droplet, leading to internal circulation patterns that can enhance the transport of heat and mass. To quantify the relative significance of this effect, the Marangoni number (Ma) is commonly employed as a dimensionless parameter. This number represents the ratio between the transport mechanisms associated with surface tension–driven convection and those governed by diffusive processes. In other words, the Ma number compares the rate of momentum and energy transport induced by Marangoni flows with the rate of transport resulting from molecular diffusion. Consequently, larger values of the Marangoni number indicate stronger surface tension–driven convection and a more pronounced influence of Marangoni effects on the overall heat transfer behavior during DWC. Figure 8 displays the change in AHF against contact angle for three diverse Ma numbers on a horizontal ($\beta = 0°$) and vertical ($\beta = 90°$) surface. As it can be seen in Figure 8, when there is no Marangoni convection ($Ma = 0$) inside the R134a liquid droplet, the growth in contact angle does not lead to an increase in AHF. In the absence of Marangoni convection, heat transfer during DWC is governed primarily by conduction through the liquid droplets, while vapor-side diffusion controls the condensation rate. Under these conditions, the contact angle influences only the droplet geometry, redistributing the liquid volume between droplet height and footprint area without significantly altering the overall thermal resistance. Although variations in contact angle modify the local conduction path length within individual droplets, these effects are geometrically compensating when averaged over the droplet population. Consequently, the effective liquid-phase thermal resistance remains nearly invariant with respect to contact angle, rendering the average heat flux insensitive to wettability in the conduction-limited regime. Only when interfacial-driven convection is present does the contact angle play a direct role in heat transfer by altering internal flow structures and advective transport. However, when $Ma = 2204$ and $\beta = 0°$, the increase in contact angle from $\theta = 100°$ to $\theta = 110°$ results in 5.5% increase in AHF. Moreover, for the case of $Ma = 11020$ and $\beta = 0°$, the value attains 21.5%. A greater Ma number results in a superior surface tension gradient and consequently a higher temperature gradient which can lead to having an increase in heat transfer coefficient and that explains why AHF at elevated Ma numbers is more compared to lower Ma numbers. As for the contact angle, when it increases the AHF increases as well since a higher contact angle results in a lower liquid-solid contact which in turn ameliorates the AHF. For the vertical surface, AHF increase by 0%, 7.1% and 25% when $Ma = 0$, $Ma = 2204$ and $Ma = 11020$, respectively. It is evident that inclination angle has a direct influence on AHF. Also, when $Ma = 11020$ and $\theta = 110°$, AHF is greater by approximately 4.5% on a vertical surface compared to a horizontal one. The droplet's footprint on a solid surface when $\beta = 90°$ is smaller than when $\beta = 0°$. To be more specific, if an equal amount of heat is going to transfer through two surfaces, the AHF for the surface with less area is undoubtedly higher. This illustrates why AHF increase with inclination angle.

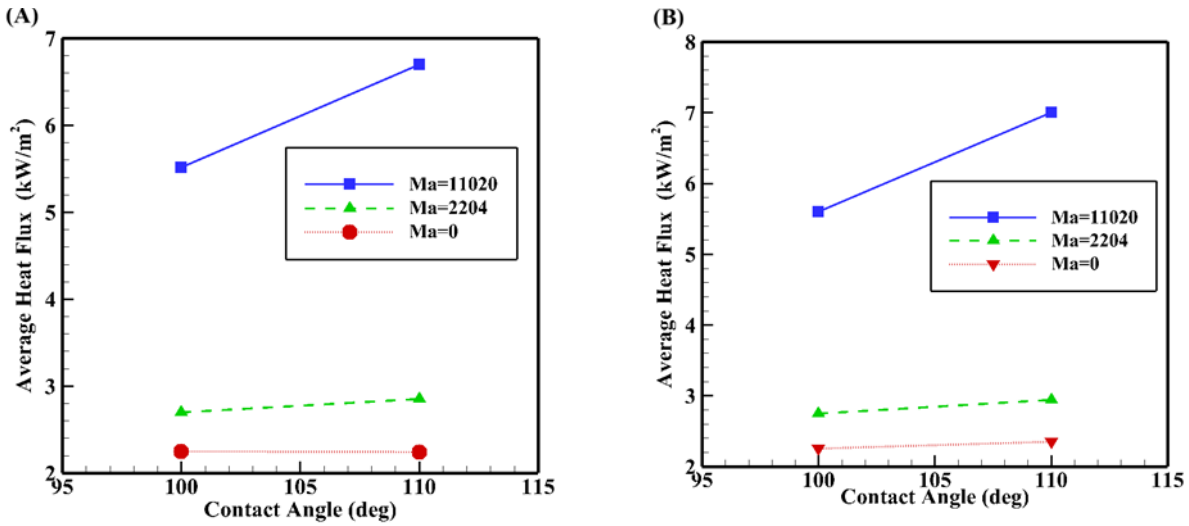

Figure 8. AHF against contact angle at diverse Ma numbers while V = 20 µl, $\hat{\sigma} = 0.01$, $\delta_w = 1$ mm, $\delta_c = 10$ µm, $K_c = 0.2$ W/m K, $K_w = 180$W/m K and $T_{sat} = 280$ K (A) $\beta = 0°$ (B) $\beta = 90°$.

3.2. The Impacts of Ma Number on Temperature Distribution across Horizontal and Vertical Surfaces

Figure 9 points out the temperature distribution inside an R134a droplet with $\theta = 110°$ on both horizontal and vertical surfaces at diverse Ma numbers. As observed, increasing the Ma number leads to a more uniform temperature distribution within the droplet. As the Marangoni number increases, surface-tension gradients along the liquid–vapor interface intensify, generating stronger interfacial shear stresses that drive internal circulation within the droplet. This Marangoni-induced flow enhances advective transport of thermal energy, which rapidly redistributes heat compared to pure conduction. When advection dominates diffusion (high Ma), temperature differences are continuously mixed by the internal flow, suppressing local thermal gradients and leading to a more spatially uniform temperature field. In contrast, at low Marangoni numbers, weak interfacial stresses result in negligible internal motion, and heat transfer remains diffusion-dominated, allowing pronounced temperature gradients to persist. Thus, increasing the Marangoni number effectively homogenizes the droplet temperature by reducing the relative importance of conductive thermal resistance. This uniformity promotes the development of internal circulating flow, which enhances the temperature gradient at the droplet vapor interface. The resulting stronger gradients contribute to an enlarged heat transfer rate. Furthermore, the temperature distribution on the vertical surface appears more uniform compared to the horizontal surface. This observation is consistent with earlier findings that demonstrated superior AHF for droplets on vertical surfaces, thus reinforcing the role of inclination angle in ameliorating heat transfer performance.

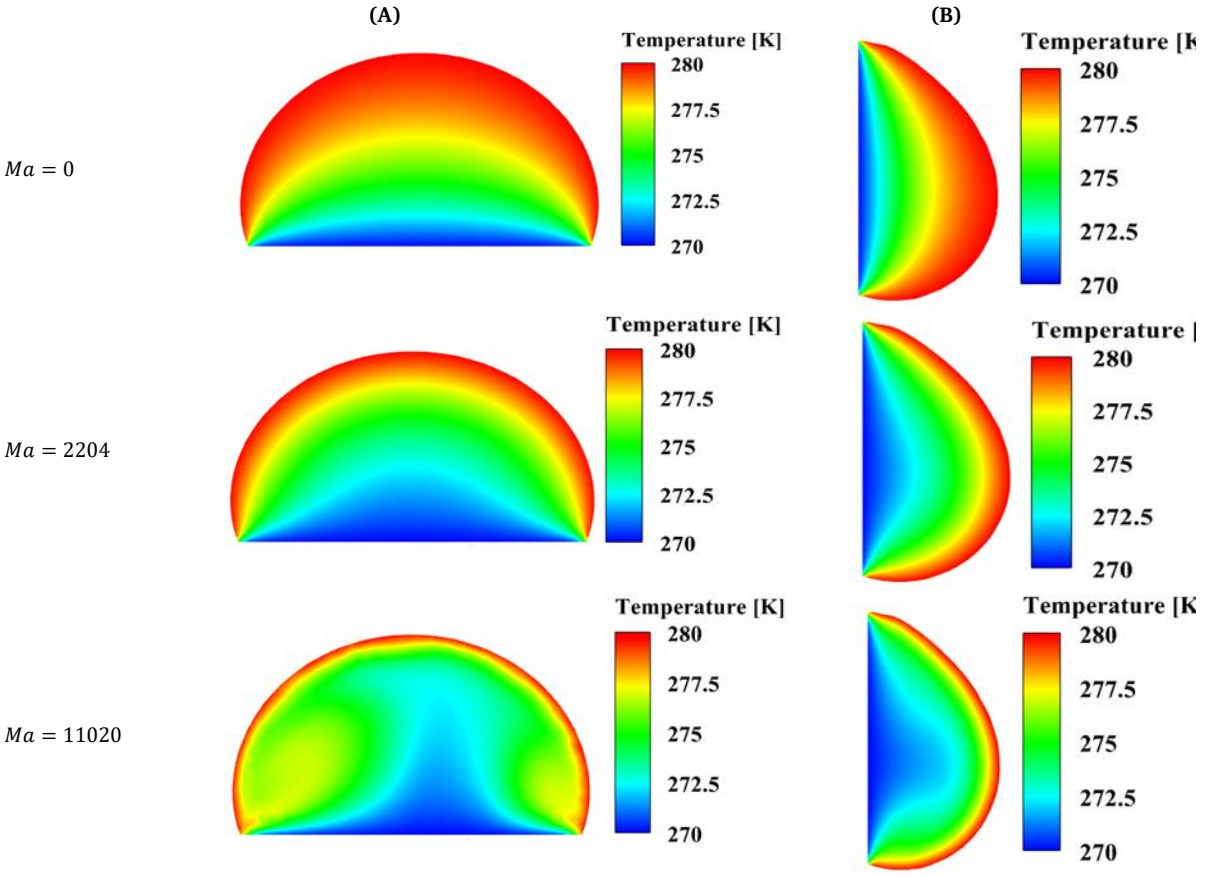

Figure 9. Temperature contours at Z-Y plane (X = 0) inside an individual R134a droplet while V = 20 µl, θ = 110°, ΔT = 10 K, T_{sat} = 280 K at three diverse Ma numbers for (A) β = 0° (B) β = 90°.

4. Conclusion

The findings of the present study demonstrate that Marangoni convection, contact angle, and surface inclination jointly exert a significant influence on the heat transfer characteristics during DWC of R134a droplets. These parameters interact to determine the internal flow structure of the droplet, the effective heat transfer area, and ultimately the overall condensation performance. An increase in the Marangoni number (Ma) strengthens thermocapillary forces generated by surface tension gradients along the liquid–vapor interface. As a consequence, stronger internal circulation develops inside the droplet, which promotes enhanced mixing and reduces temperature gradients within the liquid phase. This intensified fluid motion leads to a more uniform temperature distribution and facilitates more efficient heat transport from the vapor–liquid interface toward the solid surface, thereby increasing the overall heat transfer rate. The contact angle (θ) also plays a crucial role in determining condensation performance. Larger contact angles produce droplets with a more spherical geometry and a smaller liquid–solid contact area. Although the footprint of the droplet decreases, the associated reduction in thermal resistance and modification of heat flow paths can enhance the AHF through the droplet. The numerical results confirm that increasing the contact angle systematically improves the heat transfer capability of the droplet under the investigated conditions. For a horizontal surface configuration ($\beta = 0^{\circ}$) at Ma = 2204, increasing the contact angle from $\theta = 100^{\circ}$ to $\theta = 110^{\circ}$ results in approximately 5.5% enhancement in the AHF. When the thermocapillary effects become stronger and the Marangoni number increases to Ma = 11020, the sensitivity of heat transfer to the contact angle becomes considerably more significant, leading to an AHF improvement of about 21.5% over the same contact-angle range. A different trend is observed for the vertical surface configuration ($\beta = 90^{\circ}$). Under this orientation, the increases in AHF corresponding to the same change in contact angle are 0%, 7.1%, and 25% for Ma = 0, Ma = 2204, and Ma = 11020, respectively. These results clearly indicate that the influence of contact-angle variation on heat transfer intensifies as Marangoni convection becomes stronger, highlighting the strong coupling between thermocapillary-driven flow and droplet geometry. Furthermore, a comparison between surface orientations reveals that vertical surfaces consistently exhibit superior heat transfer performance compared with horizontal surfaces. This improvement can be attributed to the reduced droplet footprint on vertical surfaces, which leads to a more concentrated heat transfer region and a more favorable droplet geometry for thermal transport. Quantitatively, at Ma = 11020 and $\theta = 110^{\circ}$, the vertical surface provides approximately 4.5% higher AHF than the horizontal configuration. To ensure the reliability of the computational approach, the numerical model was validated against both theoretical predictions and experimental measurements reported in previous studies. The strong agreement obtained in these comparisons confirms the robustness and accuracy of the developed numerical framework. Overall, the analysis highlights that microscale droplet dynamics play a critical role in determining macroscopic condensation performance. By carefully controlling parameters such as Marangoni convection intensity, surface wettability, and surface orientation, it is possible to significantly enhance heat transfer during dropwise condensation. These insights are particularly valuable for thermal management systems and refrigeration technologies, where improved droplet-level heat transfer can contribute to higher refrigeration efficiency and reduced energy consumption.

Nomenclature

Symbols

$d\sigma/dT$	Surface Tension Gradient (N/mK)
$\left(\frac{\partial T}{\partial x_i}\right)_c$	Temperature Gradient Vector at The Condensing Surface (K/m)
g	Gravity Acceleration (m/s^2)
h_i	Interfacial Heat Transfer Coefficient $(W/m^2\,K)$
h_{lv}	Latent Heat of Vaporization (J/kg)
k	Thermal Conductivity (W/mK)
L	Droplet Height (m)
M	Vapor Molecular Weight (kg/mol)
P_v	Vapor Pressure (Pa)
q	Average Heat Flux (W/m^2)
$\bar{R}$	Universal Constant of Gases $(J/mol\,K)$
T	Temperature (K)
T_{cap}	Temperature Near Droplet Interface (K)
u	Fluid Velocity in X-Direction (m/s)
v	Fluid Velocity in Y-Direction (m/s)
w	Fluid Velocity in Z-Direction (m/s)
V	Volume of Droplet (μl)
x, y, z	Cartesian Coordinate

Greek symbols

α	Thermal Diffusivity (m^2/s)
β	Surface Inclination Angle (deg)
ρ	Condensate Density (kg/m^3)
θ	Contact Angle (deg)
μ	Dynamic viscosity $(kg/m\,s)$
σ	Surface Tension (N/m)
$\hat{\sigma}$	Condensation Coefficient
δ	Thickness (m)

Subscripts

sat	Saturation Condition

Abbreviations

CFD	Computational Fluid Dynamics
DWC	Dropwise Condensation
FWC	Filmwise Condensation
FVM	Finite Volume Method
Ma	Marangoni Number

References

[1] O. M. E. S. Khayal, et al., "Condensation Heat Transfer: Principles, Mechanisms, and Mathematical Modeling," *Excellence Journal for Engineering Sciences*, vol. 2, no. 1, 2025.

[2] L. Mohammadpour, E. Aminian, and H. Saffari, "Investigating the Effect of Marangoni Phenomenon on Single Drop Density on Wenzel and Cassie Structures," *Journal of Solid and Fluid Mechanics*, vol. 10, no. 4, pp. 387–398, 2020.

[3] D. Schurk, "The Fundamentals of Condensation," *ASHRAE Journal*, vol. 67, no. 2, 2025.

[4] Q. Peng, L. Jia, et al., "Analysis of Droplet Dynamic Behavior and Condensation Heat Transfer Characteristics on Rectangular Microgrooved Surface with CuO Nanostructures," *International Journal of Heat and Mass Transfer*, vol. 130, pp. 1096–1107, 2019.

[5] A. M. Al-Tajer, W. H. Alawee, H. A. Dhahad, K. A. Hammoodi, and Z. M. Omara, "Assessing the Environmental Impact of Innovative Hybrid Desalination and Atmospheric Water Harvesting Technologies," *Journal of Thermal Analysis and Calorimetry*, vol. 150, no. 20, pp. 16735–16752, 2025.

[6] Z. Wang, T. Horseman, et al., "Pathways and Challenges for Efficient Solar-Thermal Desalination," *Science Advances*, vol. 5, no. 7, 2019.

[7] V. P. Carey, *Liquid-Vapor Phase-Change Phenomena: An Introduction to the Thermophysics of Vaporization and Condensation Processes in Heat Transfer Equipment*, CRC Press, 2020.

[8] W. Ji, G. Chong, C. Zhao, H. Zhang, and W. Tao, "Condensation Heat Transfer of R134a, R1234ze(E) and R290 on Horizontal Plain and Enhanced Titanium Tubes," *International Journal of Refrigeration*, vol. 93, pp. 259–268, 2018.

[9] P. Dehghani, S. M. Hosseinalipour, and H. Akbari, "Investigating the Effect of Environmental Conditions and Surface Type on Condensation Heat Transfer Coefficient and Droplet Departure Time," *International Journal of Thermal Sciences*, vol. 208, 109466, 2025.

[10] M. Afshari, H. Moghadasi, and L. Mohammadpour, "Assessing Parameters Impact in Dropwise Condensation Heat Transfer for an Individual Droplet on Inclined/Grooved Surfaces: a Sobol Sensitivity Analysis," *Scientific Reports*, vol. 15, no. 1, 2025.

[11] H. Chen, C. Shi, et al., "Investigation of the Droplet Dynamics and Thermal Performance During Dropwise Condensation in the Wickless Heat Pipe Condenser," *International Communications in Heat and Mass Transfer*, vol. 161, 108487, 2025.

[12] E. Schmidt, W. Schurig, and W. Sellschopp, "Versuche Über Die Kondensation Von Wasserdampf in Film- Und Tropfenform," *Technische Mechanik und Thermodynamik*, vol. 1, no. 2, pp. 53–63, 1930.

[13] L. Mohammadpour, H. Moghadasi, and H. Saffari, "Computational Fluid Dynamics Investigation of Dropwise Condensation Heat Transfer Through a Single Droplet on Wenzel Structures," *International Communications in Heat and Mass Transfer*, vol. 145, 106853, 2023.

[14] L. Mohammadpour, H. Moghadasi, and A. Moosavi, "The Influence of Nusselt Number on Dropwise Condensation Heat Transfer for a Single Droplet on Inclined and Grooved Surfaces," *Scientific Reports*, vol. 15, no. 1, 2025.

[15] P. Varshney, S. Mohapatra, and A. Kumar, "Fabrication of Mechanically Stable Superhydrophobic Aluminium Surface with Excellent Self-Cleaning and Anti-Fogging Properties," *Biomimetics*, vol. 2, no. 1, 2, 2017.

[16] Y. Huang, D. Sarkar, and X. Chen, "A One-Step Process to Engineer Superhydrophobic Copper Surfaces," *Materials Letters*, vol. 64, no. 24, pp. 2722–2724, 2010.

[17] S. Abedinnezhad, M. Ashouri, C. Chhokar, and M. Bahrami, "Natural Dropwise Condensation of Humid Air on Engineered Flat Surfaces: An Experimental Study," *Energy*, vol. 316, 134412, 2025.

[18] K. Chen, P. Gao, et al., "Theoretical Analysis of Condensation Heat Transfer Enhancement on Dot-Matrix Hydrophilic-Hydrophobic Composite Surfaces: Hydrophobic Shapes and Surface Inclination Effect," *International Communications in Heat and Mass Transfer*, vol. 169, 109568, 2025.

[19] C. Chu, X. Zhou, et al., "How Can Dropwise Condensation Be Achieved on Superhydrophobic Nanocones?," *Soft Matter*, vol. 21, no. 33, pp. 6584–6595, 2025.

[20] V. K. Dhir, and G. Son, "Film and Dropwise Condensation," *Phase Change Heat Transfer*, pp. 216–242, 2025.

[21] M. Tancon, A. Abbatecola, et al., "Investigation of Surface Inclination Effect During Dropwise Condensation of Flowing Saturated Steam," *International Journal of Thermal Sciences*, vol. 196, 108738, 2024.

[22] V. Baghel, B. S. Sikarwar, and K. Muralidhar, "Modeling of Heat Transfer Through a Liquid Droplet," *Heat and Mass Transfer*, vol. 55, no. 5, pp. 1371–1385, 2018.

[23] L. Mohammadpour, H. Moghadasi, and H. Saffari, "Numerical Scrutinization of Dropwise Condensation Heat Transfer on an Inclined Surface," *Heat Transfer*, vol. 51, no. 5, pp. 4667–4687, 2022.

[24] A. Obeidat, and H. M. Ali, "Marangoni Condensation of Steam-Ethanol Mixture on Wire-Wrapped Tube: Effect of Wire Pitch on Heat Transfer Augmentation," *International Journal of Thermal Sciences*, vol. 214, 109912, 2025.

[25] A. Phadnis, and K. Rykaczewski, "The Effect of Marangoni Convection on Heat Transfer During Dropwise Condensation on Hydrophobic and Omniphobic Surfaces," *International Journal of Heat and Mass Transfer*, vol. 115, pp. 148–158, 2017.

[26] J. Guadarrama-Cetina, et al., "Droplet Pattern and Condensation Gradient around a Humidity Sink," *Physical Review E*, vol. 89, no. 1, p. 012402, 2014.

[27] B. S. Sikarwar, K. Muralidhar, and S. Khandekar, "Effect of Drop Shape on Heat Transfer During Dropwise Condensation Underneath Inclined Surfaces," *Interfacial Phenomena and Heat Transfer*, vol. 1, no. 4, pp. 339–356, 2013.

[28] K. A. Brakke, "The Surface Evolver," *Experimental Mathematics*, vol. 1, no. 2, pp. 141–165, 1992.

[29] B. Chen, J. Tian, R. Wang, and Z. Zhou, "Theoretical Study of Cryogen Spray Cooling with R134a, R404A and R1234yf: Comparison and Clinical Potential Application," *Applied Thermal Engineering*, vol. 148, pp. 1058–1067, 2019.

[30] J. Tian, L. Kong, et al., "Experimental Investigation on Heat Transfer Performance During Electrospray Cooling with Ethanol–R141b Mixture," *Applied Thermal Engineering*, vol. 230, 120879, 2023.

[31] J. J. Valencia, and P. N. Quested, "Thermophysical Properties," *Metals Process Simulation*, pp. 18–32, 2010.

[32] S. Ravi Annapragada, J. Y. Murthy, and S. V. Garimella, "Droplet Retention on an Incline," *International Journal of Heat and Mass Transfer*, vol. 55, no. 5-6, pp. 1457–1465, 2012.

[33] M. R. Rajkumar, A. Praveen, R. Arun Krishnan, L. G. Asirvatham, and S. Wongwises, "Experimental Study of Condensation Heat Transfer on Hydrophobic Vertical Tube," *International Journal of Heat and Mass Transfer*, vol. 120, pp. 305–315, 2018.

Declaration of competing interest

The authors declare that they have no known competing financial interests or personal relationships that could have appeared to influence the work reported in this paper. The ethical issues, including plagiarism, informed consent, misconduct, data fabrication and/or falsification, double publication and/or submission, redundancy, have been completely observed by the authors.

Bibliography

Loghman Mohammadpour received his M.Sc. degree in Mechanical Engineering from Iran University of Science and Technology, Tehran, Iran, in 2018. His research interests include energy condersion systems, computational fluid dynamics, fluid mechanics, dropwise condensation, porous media and heat transfer.
Email: loghmanmo92@gmail.com
ORCID: 0000-0003-4453-7320
Contribution Statement: Conceptualization, Data curation, Formal analysis, Investigation, Methodology, Software, Writing - original draft.

Hesam Moghadasi received his Ph.D. degree in Mechanical Engineering from Iran University of Science and Technology, Tehran, Iran, in 2022, and his Postdoc Fellow from Sharif university of technology, Tehran, Iran, in 2024. He was visiting researcher in department of Mechanical Engineering at Technical University of Denmark, Copenhagen, Denmark. He is currently an Assistant Professor at Department of Mechanical Engineering, Faculty of Engineering, Arak University, Arak, Iran. His research expertise lies in energy conversion systems, heat transfer amelioration, multiphase flow, computational fluid dynamics, nanofluids, renewable energy, surface science, boiling and condensation.
Email: h-moghadasi@araku.ac.ir
ORCID: 0000-0002-9149-7272
Contribution Statement: Conceptualization, Formal analysis, Investigation, Methodology, Supervision, Writing-review & editing.